The Australian Plasma Fusion Research Facility: Recent Results and Upgrade Plans

B. D. Blackwell [1], D.G. Pretty [1], J. Howard [1], S.T.A. Kumar [2], R. Nazikian [3], J.W. Read [1] C.A. Nuhrenberg [4], J. Bertram [1], D. Oliver [5], D. Byrne [1], J.H. Harris [6], M. McGann [1], R.L. Dewar [1], F. Detering [7], M. Hegland [8], S. Haskey [1], M. J. Hole [1].

1) Plasma Research Laboratory, The Australian National University, ACT 0200, Australia.
2) Present Address: Department of Physics, University of Wisconsin-Madison, USA.
3) Princeton Plasma Physics Laboratory, NJ, USA.
4) Max-Planck-Institut für Plasmaphysik, Greifswald
5) Present Address: Research Group, Boronia Capital, Sydney Australia
6) Oak Ridge National Laboratory, Tn, USA.
7) Diversity Arrays Technology Pty Ltd, Yarralumla, ACT 2600, Australia.
8) Mathematical Sciences Institute, The Australian National University, ACT 0200, Australia.

e-mail contact of main author:: boyd.blackwell@anu.edu.au

Abstract: The "flexible Heliac" coil set of helical axis stellarator H-1 (major radius R=1m, and average minor radius <r> ~ 0.15-0.2 m) permits access to a wide range of magnetic configurations. This has enabled investigation of the effect of plasma configuration on Alfvénic range instabilities, magnetic island studies, and the development of a number of innovative imaging and 2D diagnostics. Alfvén modes normally associated with energetic populations in larger scale fusion experiments are observed, in the absence of any obvious population of energetic particles. Using H-1's unique combination of flexibility and variety of advanced diagnostics RF-generated plasma in H-1 is shown to have a very complex dependence on configuration of both the electron density and the nature of fluctuations in the MHD Alfvén range. The magnetic fluctuations range from highly coherent, often multi-frequency, to approaching broad-band (df/f ~ 0.02-0.5), in the range 1-200kHz. Application of datamining techniques to a wide range of configurations classifies these fluctuations and extracts poloidal and toroidal mode numbers, revealing that a significant class of fluctuations exhibit scaling which is i) Alfvénic with electron density (within a constant factor) and ii) shear Alfvénic in rotational transform. An array of optical and interferometric diagnostics is combined with the magnetic probe arrays to provide initial information on the internal structure of the MHD modes, and associated 3D effects. The configurational dependence is closely related to the presence of low order rational surfaces; density falls to very low values near, but not precisely at these rational values. Results from a uniquely accurate magnetic field mapping system, combined with a comprehensive model of the vacuum magnetic field in H-1 show that magnetic islands should not dominate the confinement of the configuration, and indicate that the strong dependence of plasma density on configuration may be attributable to variations in plasma generation favouring the presence of islands. Magnetic islands have been deliberately induced to study their effect on lower temperature plasma to allow the use of Langmuir probes. It was found that islands can cause both flattening and peaking in the plasma density profile. Finally, plans for a significant upgrade are described, including improved heating, vacuum and diagnostic systems. A "satellite" linear device will be constructed employing helicon heating in hydrogen with a target density of 10^{19}m^{-3}. The main aim of this device is to develop diagnostic techniques on fusion-relevant advanced materials under conditions of high plasma and power density.

1. Introduction

H-1 [1] is a medium sized helical axis stellarator of major radius R=1m, and average minor radius <r> ~ 0.15-0.2 m. Its flexible heliac[2] coil set (Figure 1) permits access to a wide range of magnetic configurations, both favourable and unfavourable, achieved by precise control of the ratio k_h of the helical winding current to the ring coil current, and two sets of vertical field coils. This provides rotational transform ꞓ in the range
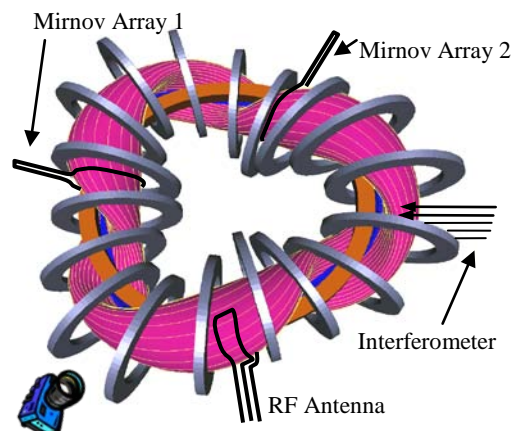

Figure 1: H-1 plasma showing location of Mirnov arrays, RF antenna, camera and interferometer; and 18 of 36 TF coils

0.9 < ṱ0 < 1.5 for B0 <1T, shear in the transform of both the positive sign typical of stellarators, and negative or tokamak-like, and magnetic well from ~5% to -2% (i.e. hill). RF-generated plasma shows a very complex dependence on configuration[3];
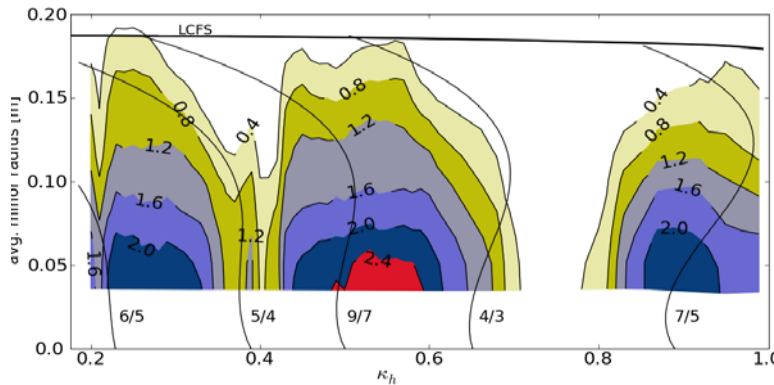
**Figure 2:** *Contours of plasma density radial profile as configuration is varied.*
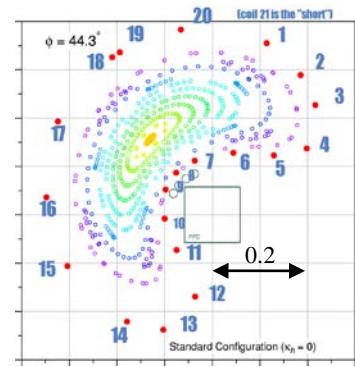
Figure 3 *Coil position (1-20) and plasma at ϕ =44.3°*

both the electron density (Figure 2) and the nature of fluctuations vary in a manner correlated with the presence of low order rational values of rotational transform. Under these conditions (H/D/He mixtures, B_0~0.5, n_e~$10^{18}m^{-3}$), signals range from highly coherent, often multi-frequency in sequence or simultaneously, to approaching broad band ($\delta f/f$ ~ 0.02-0.5), in the range 1-200 kHz, the higher frequency fluctuations (f>15 kHz) predominantly magnetic with amplitudes ~ 1gauss.

2. Magnetic Fluctuations

Data from two arrays (Figure 3) of 20 magnetic probes and several other individual probes, for a series of ~80 magnetic configurations in the range 1.1 < ṱ0 < 1.4 provides much information about the nature of these instabilities, but amounts to a formidable data set. Data mining techniques[4] allow automated processing using Fourier and SVD[5] techniques, in the time domain and in space respectively, reducing the multi-channel timeseries data to a much

smaller set of "fluctuation structures" on a much coarser time grid, characterised by a dominant frequency, amplitude, and relative phase of magnetic probe channels. At this level, data from hundreds of shots can be rapidly searched in an SQL database on a desktop computer, and datasets of the entire history of a device can be searched on a supercomputer.

Further data filtering typically involves entropy and/or energy thresholds, and classification of similar phenomena by clustering[6] in the multi-dimensional (15-40) space of phase difference between adjacent coils. This effectively
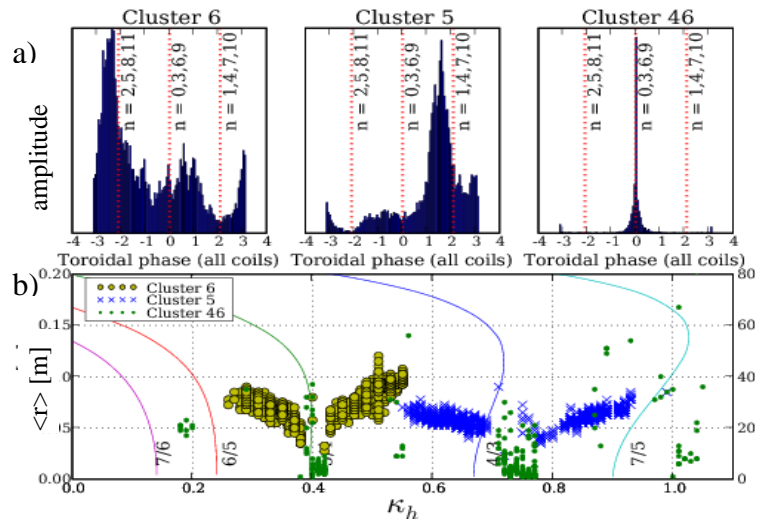
Figure 4: *Results of the classification of the configuration scan (k_h). Three of the clusters found are shown, Cluster 6 with mode numbers n/m=5/4, cluster 5 (n/m=4/3) and cluster 46 with n=0. In b), the mode frequency is shown, and thin lines are contours of rational rotational transform as a function of radius.*
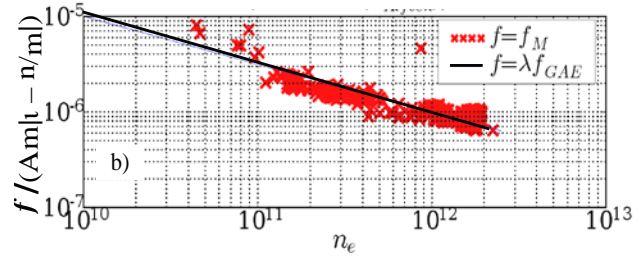
groups according to mode numbers, both toroidal and poloidal, without the need for spatial Fourier analysis. Avoiding spatial Fourier analysis is a significant advantage in the strongly toroidal geometry of compact devices, or in the three dimensional geometry typical of stellarators where mode structure is far from sinusoidal. To some degree this enables the analysis to adapt to magnetic

Figure 5: Reduced data showing clear Alfvénic dependence on 1/√ne.

coordinate systems which vary with the plasma configuration. This analysis is illustrated in Figure 4, which shows three clusters of data points with distinct mode structure.

A significant class of fluctuations (such as clusters 5 and 6, Figure 4) exhibit scaling which is Alfvénic with electron density (within a constant factor λ) as illustrated in Figure 5, and shear Alfvénic in rotational transform as will be shown in the next section.
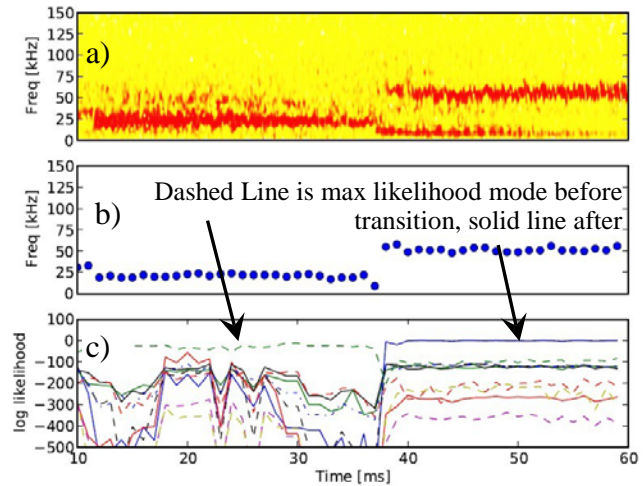
Having identified these clusters, probability density in the multi-dimensional space of nearest neighbour phase difference can be used to quickly identify modes in new data. This is shown in Figure 6, where a very large difference in the ordering of (log) probability of the modes involved in the activity before and after ~37ms clearly shows the clusters to which the two dominant modes belong.

Figure 6: Spectrogram of MHD fluctuations in H-1, showing a) mode transition, b) mode extraction and c) identification.
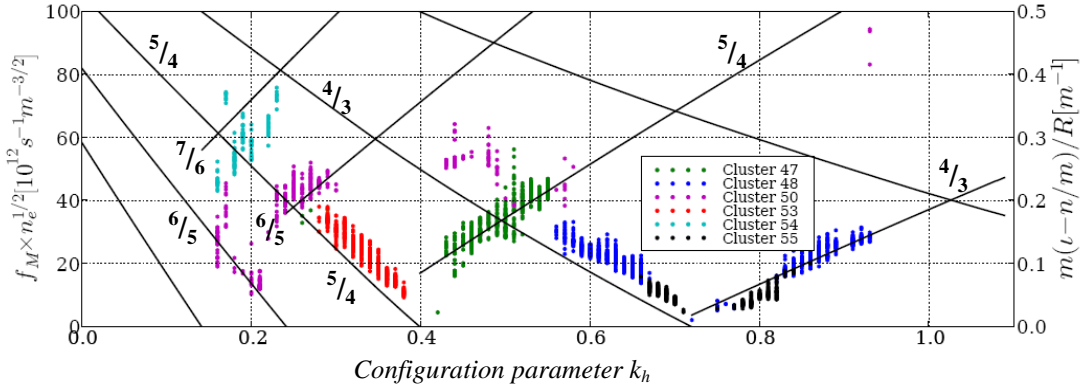
2.1 Interpretation

The analyses and clustered data of Figure 7 may be interpreted in terms of interaction between the periodic boundary conditions in a torus and the closeness of the twist number of the magnetic field lines to the ratio of toroidal to poloidal mode numbers. In low shear configurations near (but not at) resonance, global Alfvén eigenmodes (GAEs) [7] are predicted to cluster in the spectral gap $0<\omega<|k_{\parallel}V_A|$ which decreases as the transform approaches resonance ($\iota = 5/4$ and $4/3$), and which would lead to minima in f as follows. The Alfvén resonant frequency for the low positive shear typical of H-1 is approximately constant near the axis, and rises steeply toward the plasma edge. Using periodic boundary conditions to close the torus, then $k_{\parallel} = (m/R_0)(\iota - n/m)$, so $\omega \rightarrow 0$ linearly in the vicinity of a resonance ($\iota = n/m$). Observed frequencies are proportional to $\omega/V_A = k_{\parallel} = (m/R_0)(\iota - n/m)$ and, by virtue of the linear dependence on ($\iota - n/m$) either side of the minimum (~0) in ω at resonance (rational $\iota = n/m$), show clear "V" structures near those rational surfaces. In addition to their intrinsic interest, in a low shear device such as H-1, it will be shown below that these features can provide an accurate location of resonant surfaces under plasma conditions, which agree very well with recent magnetic field line mapping at high magnetic field.
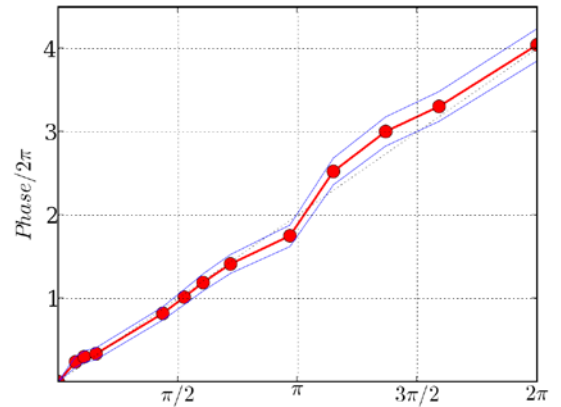
Figure 7: *A more complete data set re-scaled by $\sqrt{n_e}$ to show Alfvenic dependence on configuration parameter k_h. Lines show expected Alfven frequency at the stationary point in rotational transform profile when the corresponding resonance is in the plasma, and at a fixed radius ($<a> \sim 15cm$) if not.*
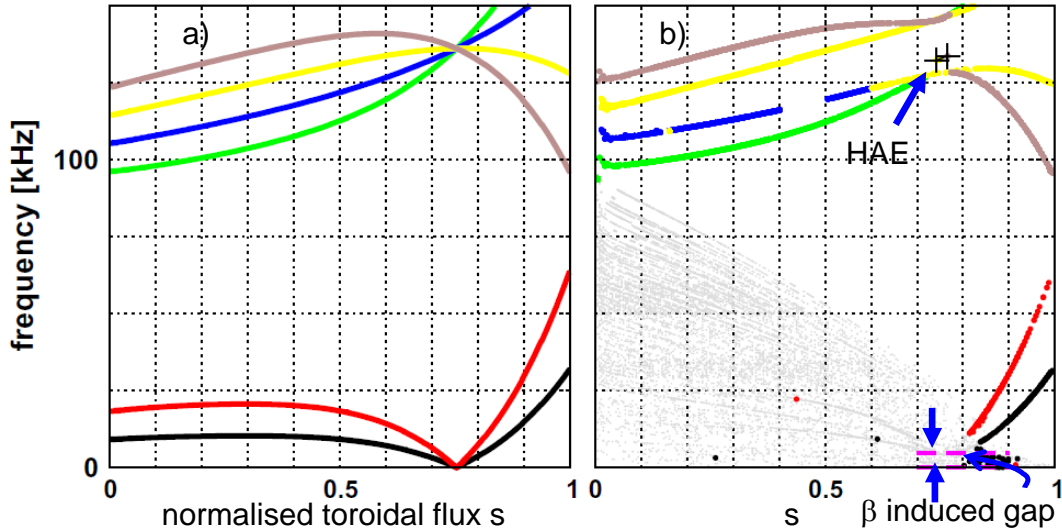
Figure 7 shows a more complete data set scaled to remove electron density variations, assuming Alfvénic scaling, and with lines for selected modes (n/m) showing the expected Alfvén frequency for a cylindrical model at the location of zero shear in the iota profile, which is approximately the condition for an Alfvén eigenmode. A better match to experimental data is found if this condition is modified so that when the corresponding resonance condition $\iota = n/m$ is not met at any radius (such as the right branch of the 5/4 mode : $0.4 < k_h$), the iota value is taken at a radius $<a> = 15cm$, near the plasma edge. Figure 10 supports this; maximum fluctuation amplitude is further from the axis for the 5/4 range than the 4/3 range of modes. The identification of the 7/6 and 6/5 modes is not as certain as they are closer to the Nyquist spatial frequency of the 20 coil arrays when the "distortion" of the magnetic coordinate system is taken into account.

The poloidal phase variation shown in Fig. 8 confirms the mode number m=4, and the approximately linear dependence of phase indicates a rotating mode in the ion diamagnetic direction. Although many of the identified modes have this rotation direction, the linearity of the phase is not as consistent as in Heliotron J using the same analysis. This is possibly a consequence of the more marked departure from circularity of the cross-section of H-1.

Fig. 8: Phase variation of the modes in cluster 6 with poloidal angle, showing a mode number m=4. The red line and points show the cluster means, and the thin blue lines the standard deviation within the cluster.

Although the dependence on iota (ι - n/m) is clear, absolute frequency values are lower than predicted by a constant scale factor λ of 1/3. This could be caused by the effective mass density being higher than that of the constituent gas mix due to impurities or momentum transfer to background neutrals, but the extent of both these effects is expected to be too small to explain the entire factor. There is a report[8] of an instability driven by fast particles travelling at velocity reduced by a comparable scale factor (1/3) and an observation[9] of a toroidal Alfvén eigenmode with spectral components at 1/3 the expected frequency, but the physical mechanism is not clear, and the experimental conditions are somewhat different. The resonant (bounce) condition in the intricate stellarator geometry is more complex, particularly as the q is low, the velocity necessary to drive the instability is likely to be even less than $V_{Alfvén}/3$.

Fig. 9: *CAS3D cylindrical (a) and 3D (b) frequency spectra. They grey dots are sound mode continua for high mode numbers, which need to be included for convergence, especially in H-1 which has a non-negligible mirror (bumpy) component in the 1/B^2 spectrum.*

Initial computational studies using CAS3D[10] indicate that the 3D global modes and associated continua (Fig. 9) are largely unchanged in frequency from the simple cylindrical model used in the above analysis, with the exception of modes near gaps (HAE in Fig. 9) and those near zero frequency. These low frequency modes are up-shifted by a β-induced gap ~5kHz, in spite of the low β ~ 0.018%. This frequency is typical of the lower limit of modes observed with clearly resonant mode numbers. In Figure 4 for example, although the observed frequencies approach zero near the 4/3 and 5/4 resonances, the modes lose their m=3 or 4 character below about 10 kHz and show very much reduced poloidal variation in phase. The nature of the mode is more electrostatic, and together with the mode number change, is suggestive of the Beta-induced Alfvén Eigenmode (BAE) or the related Geodesic Acoustic Mode (GAM).

Recent analysis of the low frequency Alfvén–acoustic regime has found new global eigenmodes, called beta–induced Alfvén–acoustic eigenmodes (BAAE), existing in gaps in the Alfvén–acoustic continuum [11]. Through introduction of sideband coupling between m and m ± 1 modes, a generalised dispersion relation with three roots can be formed. Two roots, an acoustic sideband and a modified shear Alfvén wave, form a gap in which the BAAE resides; the other root is related to the BAE and becomes the GAM in the high–β limit, and the usual shear Alfvén wave in the low–β limit.

Theoretical treatment of the Alfvén–acoustic eigenmodes has recently been extended to low-beta, low-shear stellarator plasmas [12], where numerical calculations for HSX yielded weakly damped BAAE modes with comparable frequencies to HSX experimental results.

Returning to the HAE mentioned in relation to Fig. 9, there is some evidence of a mode of this type, but at a higher rotational transform. At rotational transform approaching 1.4-1.5, there is a cluster of modes (Fig. 11) which are non-resonant, and with frequency dependence which matches that expected from another Helical Alfvén Eigenmode (HAE), but with a scale factor λ much closer to unity (0.85) . Although encouragingly close to unity, this is inconsistent with the scale factor required for agreement with theoretical frequencies of resonant modes in Figure 7.
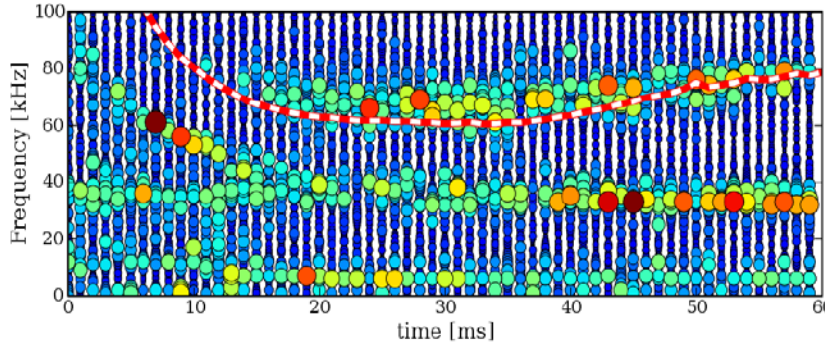
Fig. 10: *Uppermost mode cluster (red dashed line) exhibits Helical Alfvén Eigenmode scaling as density varies in time for one plasma discharge.*

2.2 Radial Mode Structure

The radial localisation of the fluctuations has been investigated with a precision 2mm interferometer and a 1.5mm fast scanning interferometer[13]. Figure 10 shows the chordally integrated fluctuation amplitude as a function of configuration parameter k_h. The mode near the 5/4 resonance is seen to exist at $r < r(\iota=5/4)$ for $0.29 < k_h < 0.38$, while the mode near $k_h \sim 0.5$ has a radial fluctuation profile consistent with localisation in the zero-shear region. Note that because the interferometer is sensitive anywhere along its line of sight through the plasma, a mode localised at r_x in the plasma should appear between $0<r<r_x$ in Figure 11.
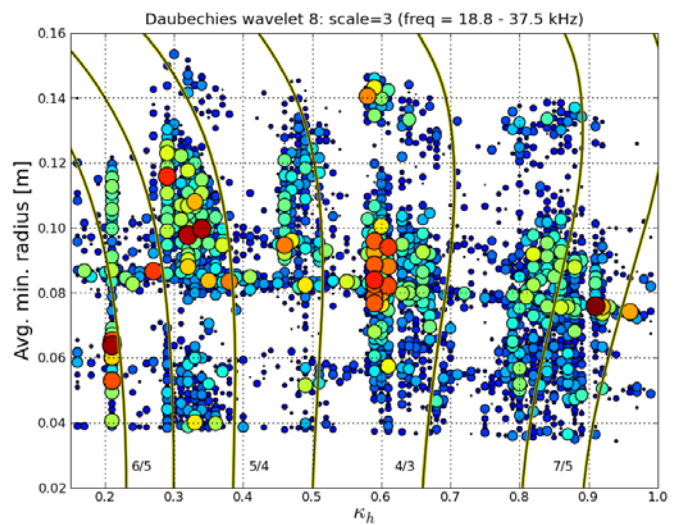
Figure 11: *Dependence of line-averaged density fluctuation amplitudes (dot size) on effective radius of the line of sight and configuration parameter k_h. The swept nature of the diagnostic causes reproducible global modes (e.g. $k_h \sim 0.6$) to be artificially broken up into separate data points.*

Mode structure simulations assuming m=3 and 4 are consistent with data and the explanation of the Alfvén eigenmodes given in §2.1. Fig. 12 shows such a simulation and the experimentally measured structure of the n=5, m=4 mode extracted by synchronous detection of the density fluctuations detected by a low-noise 2mm interferometer scanned through the plasma on a shot to shot basis. The figure shows the reproducibility of the results, and a qualitative correspondence with a simulation of an m=4 mode in the magnetic geometry of the heliac. The simulation (a) illustrates that even for rotating modes, the phase of the line integrals of electron density tend to be near 0 or π if the view lines pass through enough plasma to see $\sim 2\pi$ range of phase shift of the mode.

Under certain conditions, optical emission from the spectral lines of ions is proportional to the product of ion and electron density($\sim n_e^2$), and if the fluctuation amplitude is small relative to the background density, the optical emission is proportional to the fluctuating part of n_e. This
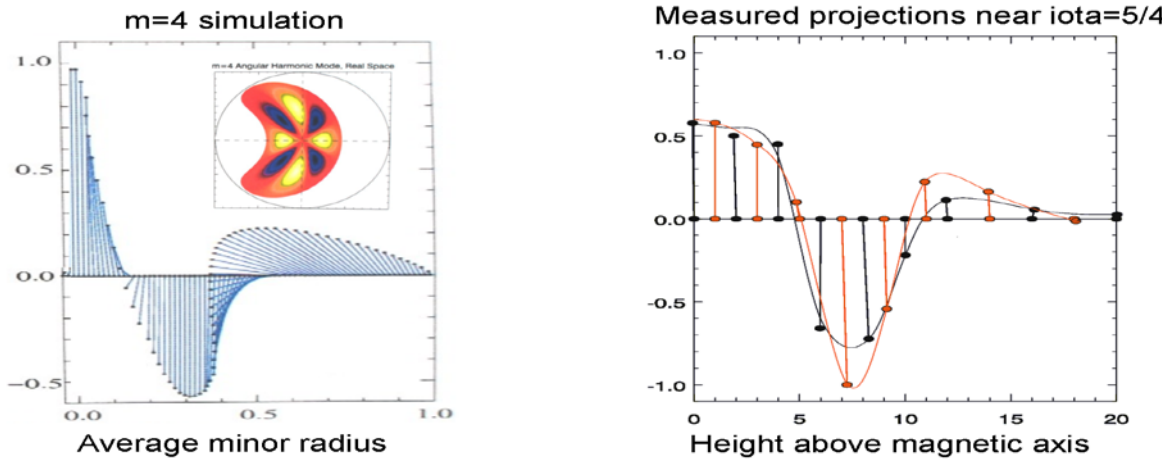
Fig. 12:a) *Simulated and b) measured mode structure in line-integral density for the stronger modes near iota=5/4 (large circles in Fig.11). The two scans shown are quite similar. The tilt of the phasors represents the phase angle. Chordal integration and symmetry causes phases to tend to 0 or π even for rotating modes.*

allows 2d measurements to be made by imaging devices such as high speed, high resolution CCD cameras.

Results from a high speed Princeton Instruments PIMAX 3 intensified camera viewing a vertical cross-section of the plasma (Figure 1) gated in synchronism with the mode are shown in Figure 13 for $\kappa_h = 0.33$. Although the configuration is slightly different, the intensity profile is remarkably similar to the measured density oscillation profile in Fig. 12, which only covers half the plasma, from the axis outwards.

A helical gap mode predicted by CAS3D for the same configuration as in Fig. 12 is shown in Figure 14. The mode is a mixture of 5/4 and 8/6, as can be seem from the image in real coordinates. The horizontal projections, corresponding approximately to the view of the camera have a simpler structure similar to both the intensity data in Figure 13 and the density fluctuation profile data in Fig. 12. This shows that under the right conditions, spectral line intensity can be used as a proxy for density fluctuation measurements. The advantage of this
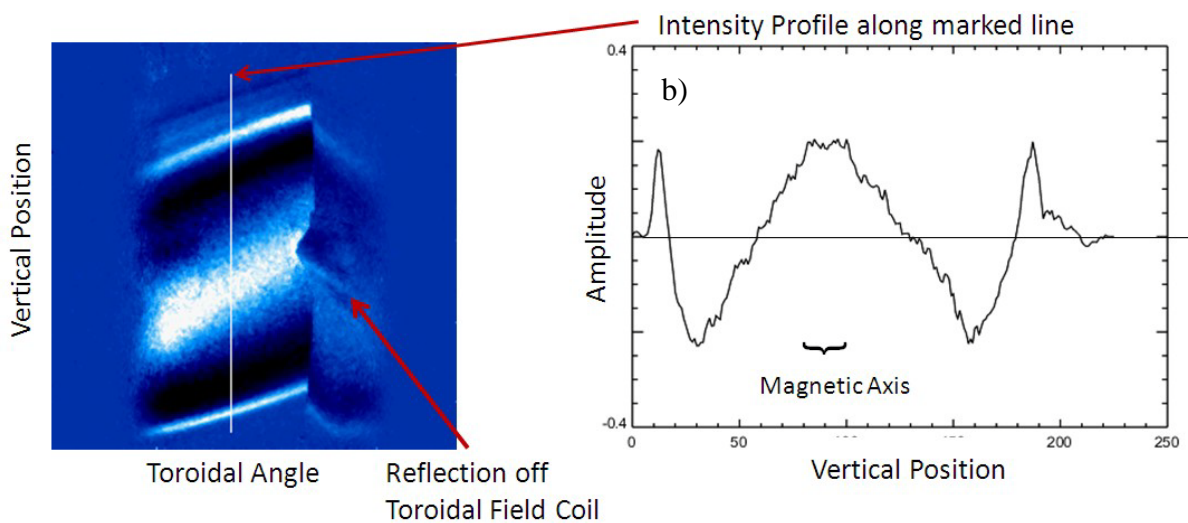
Figure 13: *Phase-resolved side view of optical emission from MHD fluctuation in H-1 viewing between the toroidal field coils. A vertical section (b) along the line indicated shows an even mode*

indirect approach is that acquisition can be automated, the camera can be moved to any port with a window and view dump, and it provides 2D data.
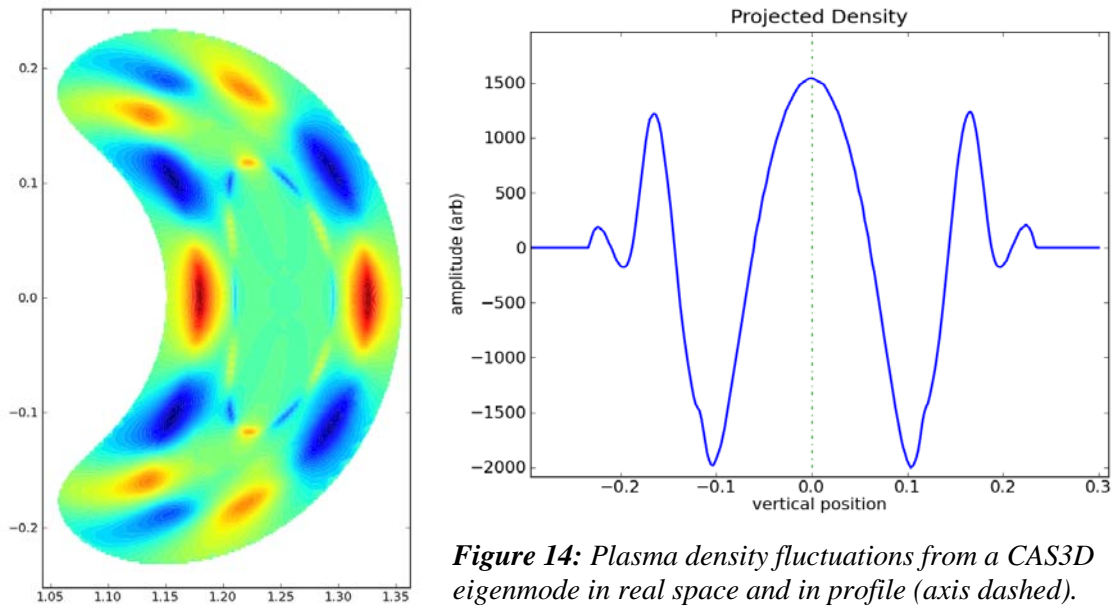
Figure 14: *Plasma density fluctuations from a CAS3D eigenmode in real space and in profile (axis dashed).*

Magnetic probe array data have also been compared with MHD predictions [14]

The complexity of the plasma shape (Figures 1, 3), and its variation with configuration creates problems in analysis, possibly broadening the poloidal mode spectrum more than expected from toroidal and helical coupling. The variable plasma – probe distance makes mode localisation difficult. Consequently, the identification of ballooning modes by comparing mode amplitudes in regions of favourable and unfavourable curvature is difficult. However there are clearly some modes which are quite different to the Alfvén eigenmodes described above, either more broadband, or with a density dependence that is clearly non-Alfvénic. The latter distinction is more obvious when the plasma density varies during a single plasma pulse, and the frequency variation is clearly not $1/\sqrt{n_e}$.

The drive for these modes is not clear; fast particle driving sources are under investigation, and include both fast electrons and minority-heated H ions. At this time, no clear evidence of suitable fast particles has been found. It is unlikely that H or He ions in H-1 could reach the energy required to match the Alfvén velocity, and there is no obvious spectral indication of high energy components either through charge exchange to H atoms or acceleration of He ions by drag from fast H ions. However both these processes are indirect, and Doppler broadened features due to such high energies would be far into the wings of the spectral lines, and may be difficult to distinguish from the background. There is a distinct possibility of acceleration of either species by the high potential RF (~kV) on the antenna, and it is common to find an elevated temperature in either or both electron and ion species near the edge in RF heated H-1 plasma[15]. Recently observations of excitation of Alfvén eigenmodes by steep temperature gradients, in the absence of high-energy tails, have been reported.[16]

3. Effects of Configuration and Magnetic Islands on Plasma Density

The plasma density falls dramatically near the resonances discussed in §2.1, leading to the question: To what extent is this due to the effect of magnetic islands? Magnetic islands are expected to be relatively less important in a heliac than in conventional stellarators because of the combination of flexibility and moderate shear – the shear is small enough so that in most configurations, there are no low order rationals present, but sufficiently large so that island width is reduced in configurations containing significant rationals. We have developed a uniquely accurate magnetic field mapping system[17] using tomography of electron beam

currents collected by a rotating wire wheel, and a comprehensive model of the vacuum magnetic field in H-1. The model includes details of coils and busses, all significant sources of magnetic field error and stray fields. The computation and electron beam mapping measurement agree well and the number of transits is sufficient for measurements of iota to better than 3 decimal places in the vicinity of moderate order resonances (m,n ~ 8-15), using the computer fit only to second order.
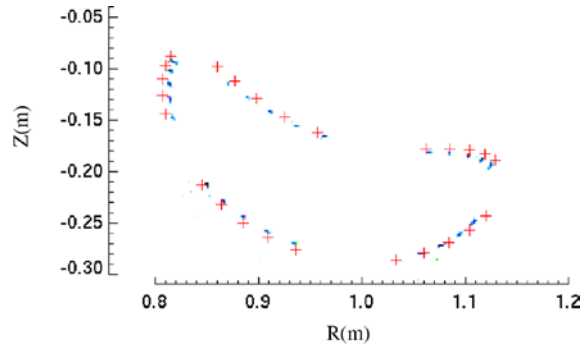
Figure 15: Measured vacuum punctures[·] and computation[+].

This allows comparison with the iota inferred from the Alfvén mode frequency measurements reversing the procedure outlined in §2. The agreement is good ($\delta\iota/\iota$ ~0.4%) when compared to direct electron beam measurements at low magnetic field.

Recently the mapping system was upgraded [18] to allow scans fast enough to allow partial imaging at full operating magnetic field. This showed a small change in iota due to helical distortion of conductors under the magnetic force loading, which when extrapolated to the conditions of Figure 16b, reduces the discrepancy to $\delta\iota/\iota$ <0.2%. This demonstrates the potential of this technique in measurement of rotational transform in the presence of plasma, provided the device has low shear, or the radial location of the mode can be clearly identified.
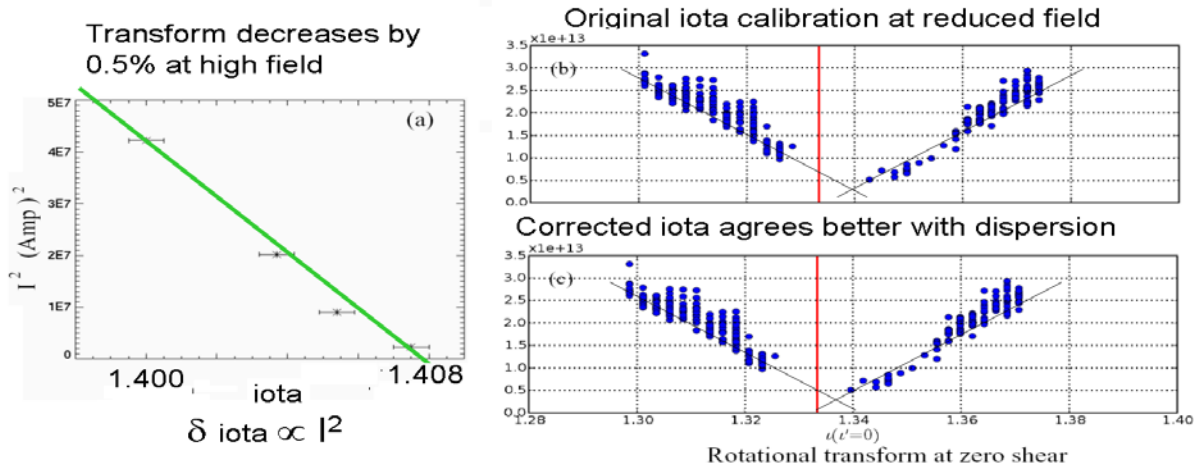
Figure 16 : Comparison of transform determination using Alfvén eigenmode resonance and direct ebeam mapping(a). The discrepancy between the transform obtained from the symmetry point in the "V" structure of the observed frequency (b) and the computed transform value is halved (c) if the computed transform is corrected for a small distortion in the magnetic field coils due to the magnetic forces inferred from the results (a) of electron beam mapping at high field.

Extensive tomographic configuration mapping and corresponding magnetic field computation shows that magnetic islands do not dominate the configuration except at iota ~ 1, and to a smaller degree at iota~3/2. The poor confinement near some resonances (Figure 2), especially

near iota values of 5/4 and 4/3, seems therefore, to be not simply due to destruction of magnetic surfaces by islands.

To allow a detailed investigation of magnetic islands, and their effect on plasma confinement, the iota~3/2 configuration was chosen because the islands inherent in the shape (elongation/indentation) of the heliac, are large enough that an effect could be expected, but not so large as to totally destroy confinement. Experiments in the vicinity of iota ~3/2 were performed in Argon plasma over a range of parameters, and do not show any clear degradation in confinement or any noticeable features at the island position (δ), as measured by Langmuir probe estimates of density and temperature. However, for lower neutral densities, there is a small increase in confinement within the island (Figure 17), and a steepening of the potential profile in the vicinity of the core. Investigations into similarity with core electron root enhanced confinement[19] are ongoing[20].

Figure 17: *Plasma density increase in presence of an island (indicated by δ) for initial neutral densities of 0.8($+$) and 1.6($*$) $10^{18}m^3$*

4. The Facility Upgrade

The Australian Government recently allocated \$7M to upgrade the facility infrastructure, including RF heating systems, vacuum quality, data access and diagnostics.
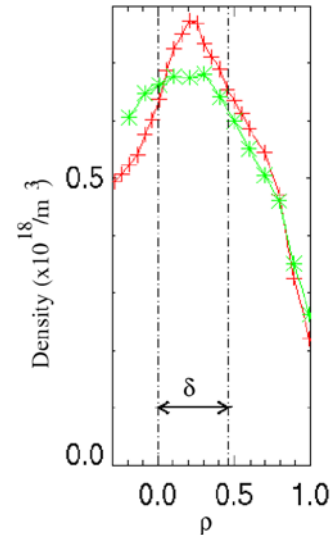
In addition to consolidating and automating some existing diagnostics, new instruments will be funded including the high speed synchronous imaging camera which produced images on previous pages, and spatially interferometric coherence imaging cameras for ion temperature and flow, and for Thomson scattering.

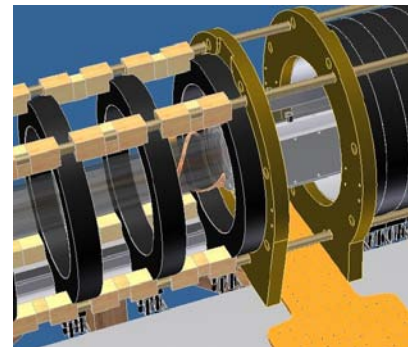### The Materials Diagnostic Development Facility

A small linear device is under construction to provide a test-bed specifically for developing and testing diagnostics for plasma-materials interaction under conditions relevant to the edge of fusion reactors. The device aims to achieve high plasma densities ($\sim 10^{19}m^{-3}$ H+) and power densities. Three different sources will be employed– an RF helicon wave source, an electron beam source and a plasma gun source. Recent results [X]show that plasma densities of $\sim 10^{19}m^{-3}$ can be achieved in hydrogen if helicon waves are launched into an increasing magnetic field.

Figure 18: *The materials diagnostic facility and b) close-up of the target chamber.*

Toroidal Mirnov Array

To complement the two existing poloidal arrays a toroidal/helical magnetic probe array has been installed, consisting of 16

Figure 19: *The Toroidal Mirnov array terminating in a special coil set enclosed in a metallised glass tube for high frequency response. The existing poloidal array is in the foreground (bean shaped tube), and CAD detail of a coils set is inset.*

sets of 3 mutually perpendicular coils housed inside a vacuum-tight thin stainless steel bellows. The bellows is essentially transparent to magnetic field in the Alfvén frequency range, and follows a toroidal helix path near the ring conductor. Proximity to the plasma produces large signal amplitudes, and traversal of regions of various magnetic curvature may enable ballooning and interchange modes to be distinguished.

5. Conclusion

We have presented strong evidence for Alfvénic scaling of magnetic fluctuations in H-1, in n_e, iota and ω. Measurements of electron density and spectral line emission have been shown to give similar results for the projection of the mode structure, which is in reasonable agreement with some initial 3D calculations for a similar configuration. There is however unclear scaling in B, and an unexplained factor of ~3 in the frequency of near-resonant modes. To clarify this, a full scan of the measured configurations is being performed with the 3D MHD code CAS3D is in progress. In low shear configurations, we have shown that near-resonant Alfvén eigenmodes can provide a sensitive iota diagnostic. The increased dimensionality of parameter space arising from such systematic investigations is efficiently handled by datamining. This technique is being applied to a number of devices internationally, coordinated through an open source software project[4]. The understanding provided by this unique combination of flexibility and variety of advanced diagnostics can contribute to the understanding of Alfvénic activity, and the effects of magnetic islands in present-day and planned extremely energetic fusion plasmas. Investigation in the influence of magnetic islands on plasma showed several interesting effects, including a local enhancement of confinement under some conditions.

The Facility upgrade includes diagnostic, data, heating, vacuum and discharge cleaning systems, and will provide access to island divertor-like configurations. A "satellite" linear device will be constructed which employs a variety of plasma formation methods, including helicon heating in hydrogen with a target density of $10^{19} m^{-3}$. The main aim of this device is to test diagnostic techniques on fusion-relevant advanced materials under conditions of high plasma and power density.

Acknowledgements

References

[1] Hamberger S.M., Blackwell B.D., Sharp L.E. and Shenton D.B. "H-1 Design and Construction", *Fusion Technol*. **17**, 1990, p 123.

[2] Harris, J.H., Cantrell, J.L. Hender, T.C., Carreras, B.A. et al. *Nucl. Fusion* **25**, 623 (1985).

[3] Harris, J.H., Shats, M.G., Blackwell, B.D., Solomon, W.M., et al. *Nucl. Fusion,* **44** (2004) 279-286.

[4] Pretty D.G, Blackwell B.D., Harris J.H *A data mining algorithm for automated characterisation of fluctuations in multichannel timeseries."* Comput. Phys. Commun., 2009. http://dx.doi.org/10.1016/j.cpc.2009.05.003. and open source code http://code.google.com/p/pyfusion/.

[5] Dudok de Wit T, Pecquet A L, Vallet JC, and Lima R. *Phys Plasmas*, **1**(10):3288-3300, 1994

[6] Witten Ian H, and Frank Eibe. Data Mining: *Practical machine learning tools and techniques.* Morgan Kaufmann, 2nd edition, 2005.

[7] Weller, A., Anton M., et al*., Physics of Plasmas*, 8 (2001) 931-956 and Wong K.L., "A review of Alfvén eigenmode observations in toroidal plasmas" *Plasma Phys. and Contr. Fusion* **41** (1): r1-56 1999

[8] Biglari H., Zonca F., and Chen L., "On resonant destabilization of toroidal Alfvén eigenmodes by circulating and trapped energetic ions/alpha particles in tokamaks" *Phys. Fluids* B 4 **8** 1992, and S Ali-Arshad and D J Campbell, "Observation of TAE activity in JET" *Plasma Phys. Control. Fusion* 37 (1995) 715-722.

[9] Maraschek, M., Günter S., Kass T., Scott B., Zohm H., and ASDEX Upgrade Team "Observation of Toroidicity-Induced Alfvén Eigenmodes in Ohmically Heated Plasmas by Drift Wave Excitation", *Phys. Rev. Lett*. **79** (1997) 4186-9

[10] C. Nuhrenberg. "Computational ideal MHD: Alfvén, sound and fast global modes in W7-AS". Plasma Phys. Control. Fusion, 41(9):1055–70, 1999.

[11] "Predictions and observations of low-shear beta-induced shear Alfvén–acoustic eigenmodes in toroidal plasmas" N.N. Gorelenkov, H.L. Berk, E. Fredrickson, S.E. Sharapov and JET EFDA Contributors http://dx.doi.org/10.1016/j.physleta.2007.05.113 Physics Letters A Volume 370, Issue 1, 8 October 2007, Pages 70-77

[12] Eremin, D.Y., Könies, A. "Beta-induced Alfv́n-acoustic eigenmodes in stellarator plasmas with low shear", (2010) Physics of Plasmas, 17 (1), art. no. 012108, .

[13]Howard J. and Oliver D., "Electronically swept millimetre-wave interferometer for spatially resolved measurement of plasma electron density", *Applied Optics* **45** (2006) pp. 8613-8620

[14] M. J. Hole *et al.*, paper presented at the this conference: FEC 2010

[15]Michael C. A., Howard J. and Blackwell B. D., "Measurements and modeling of ion and neutral distribution functions in a partially ionized magnetically confined argon plasma", *Physics of Plasmas* 75, (2004) 4180-4182.

[16]Nazikian R. et al. Phys. Rev. Lett. 96, (2006) 105006.

[17] Kumar, S.T.A, Blackwell, B.D. and Harris, J.H., "Wire tomography in the H-1NF heliac for investigation of fine structure of magnetic islands", Rev. Sci. Ins, 78 (2007) 013501-8

[18]Kumar, S.T.A and Blackwell, B.D, "Accurate determination of the magnetic geometry of the H-1NF heliac", Nuclear Fusion, 49 (2009) 035001.

[19] Yokoyama M., Maasberg H., Beidler C.D.,.et al. "Core electron-root confinement (CERC) in helical plasmas." Nucl. Fusion, 47(2007):1213–1219.

[20] S.T. Kumar, B.D. Blackwell, J. Howard and J.H. Harris, *"Core magnetic islands and plasma confinement in the H-1NF Heliac"* Phys. Plasmas, **17** (2010) in press